TH-C 1937

Advanced transport models for energetic particles

Ph. Lauber[1], M. Falessi[2], A. Biancalani[3], A. Bottino[1], S. Briguglio[2], N. Carlevaro[2], V. Fusco[2], E. Giovannozzi[2], T. Hayward-Schneider[1], F. Holderied[1], A. Könies[4], Y. Li [2,6],Y.-Y. Li[2,5,6], G. Meng[1], A. V. Milovanov[2], G. Montani[2], V.-A. Popa[1], S. Possanner[1], G. Vlad[2], X. Wang[1], M. Weiland[1], A. Zocco[1], F. Zonca[2], M. Schneider[7] and ASDEX Upgrade Team[8]

[1]*Max-Planck-Institut für Plasmaphysik, Boltzmannstraße 2, D-85748 Garching, Germany*
email: philipp.lauber@ipp.mpg.de
[2] *ENEA, Fusion and Nuclear Safety Department, C. R. Frascati, I-00044 Frascati (Rome), Italy*
[3] *Léonard de Vinci Pôle Universitaire, Research Center, F-92916 Paris La Défense, France*
[4]*Max-Planck-Institut für Plasmaphysik, D-17491 Greifswald, Germany*
[5] *National Supercomputing Center of Tianjin, Tianjin, China*
[6] *CREATE Consortium, Via Claudio 21, Napoli, Italy*
[7] *ITER Organization, Route de Vinon-sur-Verdon, CS90046, 13067 St Paul-lez-Durance, France*
[8] *see author list of U. Stroth et al 2022 Nucl. Fusion 62 042006*

Introduction

In addition to increasingly realistic non-linear global simulations [1, 2, 3, 4, 5, 6], a hierarchy of theory-based reduced models is needed to complement the predictions concerning the performance of future burning plasmas. Large parameter scans, sensitivity studies and multi-scale physics connecting energetic particle transport with neoclassical transport time scales require tools that go beyond what is presently feasible with first-principles numerical codes. In the view of this challenge we report in this work on the construction, validation and application of reduced energetic particle (EP) transport models pursued within the framework of the EUROFusion enabling research project ATEP (Advanced Transport models for EPs).

Model equations

The general theoretical framework introduces the concept of long-lived toroidally symmetric structures in the particle phase space (phase space zonal structures, PSZS) that are separated from fast fluctuating contributions [7, 8, 9, 10]. Comprehensive transport equations have been derived that are designed to capture the evolution of PSZSs on collisional transport time scales while keeping the important non-linear interactions in a consistent multi-scale description. The model captures physics beyond simpler models (critical gradient [11], kick model [12], quasi-linear [13]) that, however, can be recovered in the appropriate limits. Details and an application example for zero-frequency zonal flow generation by geodesic acoustic modes can be found in [9, 10] (at this conference). The extension to 3D geometry has been started [14].

The newly developed ATEP code is based on this PSZS transport formulation. Although in its first stages it will not comprise the full non-linear phenomenology contained in the theoretical model, its formulation and implementation are designed to capture non-linear effects in a systematic and transparent way. In its simplest limit without sources, sinks and collisions, the transport equation is formulated as a continuity (advection) equation of the EP distribution function F_z in constants of motion (CoM) phase space (P_ϕ, E, Λ) [15]:

$$\frac{\partial F_z}{\partial t} = -\frac{\partial}{\partial P_\phi}\left(\langle\overline{\frac{dP_\phi}{dt}}\rangle F_z\right) - \frac{\partial}{\partial E}\left(\langle\overline{\frac{dE}{dt}}\rangle F_z\right) \tag{1}$$

Here, P_ϕ is the canonical toroidal momentum, E the energy and $\Lambda = \mu B_0/E$ and μ the adiabatically invariant magnetic momentum. $\overline{\langle\rangle}$ indicates orbit and phase (between particles and wave) averaging. (Note that notations and definitions deviate slightly from ref. [9]). If the initial F_z is assumed to be an equilibrium state described in CoM coordinates, it will remain a zonal state (i.e.

independent of any poloidal or toroidal angle) since the phase space flow induced by the flow velocity $\mathbf{v}_{P_\phi,E} = (\langle\overline{\frac{dP_\phi}{dt}}\rangle, \langle\overline{\frac{dE}{dt}}\rangle)$ is orbit averaged. If dissipative effects are neglected the flow is incompressible and $\nabla \cdot \mathbf{v}_{P_\phi,E} = 0$.
Within the kick-model limit we assume that $\mathbf{v}_{P_\phi,E}$ is determined by a (low frequency) fluctuation spectrum with fixed amplitudes, e.g. provided by experimental measurements, comprehensive code results or a theoretical closure model. That leads to a 2D advection equation with constant advection velocity $\mathbf{v}_{P_\phi,E}$. Evolving eqn. (1) corresponds to a forced-driven system, where the externally given advection velocities flatten (or also steepen) the phase space gradients. If a physical, linearly unstable mode with fixed amplitude (i.e. a prescribed $\delta B/B$) is chosen to determine $\mathbf{v}_{P_\phi,E}$, phase space (particle) density is flowing proportional to the derivatives of F_z across the phase space volume elements. Clearly, phase space density is conserved, but within the kick-model the total energy $\mathscr{E}(t) = \int dv_{P_\phi,E,\Lambda} E \cdot F_{EP}(t)$ is not conserved. Monitoring the change in total energy allows one to determine if the perturbations have exhausted the free energy available by flattening F_z, or if the perturbation is starting to pile up energy in an unphysical way. $dF_z/d\mathscr{E} = 0$ determines the relaxed state of F_z within this model.
Clearly, for a steady-state solution, one needs to balance this relaxation with sources and sinks. The required neoclassical physics elements have been added to eqn. (1) and first promising results, using a bounce averaged collision operator in the same CoM formulation and code framework are reported in ref. [16] (at this conference).
In order to construct a quasi-linear model, an energy balance between wave amplitude spectrum and phase space flows has to be introduced [15]:

$$\frac{d}{dt}\left(\mathscr{E} + \sum_k W_k\right) = -2\sum_k \gamma_{d,k} W_k \tag{2}$$

Here, $\sum_k W_k$ is the total wave energy as a superposition k linear eigenmodes, and $\gamma_{d,k}$ their respective damping rates. Once the change of $\mathscr{E}$ has been calculated for an initial (small) wave spectrum amplitude $\delta B_0/B$ via $\mathbf{v}_{P_\phi,E}(\delta B_0/B)$, the new wave energy can be determined, leading to dynamically changing $\mathbf{v}_{P_\phi,E}(\delta B(t)/B)$. This requires to know how $(\langle\overline{\frac{dP_\phi}{dt}}\rangle, \langle\overline{\frac{dE}{dt}}\rangle)$ behave as a function of the perturbation amplitude. This system by construction conserves phase space density and total energy, if mode damping is ignored or properly accounted for in the energy balance. If the wave spectrum is not allowed to change its shape, i.e. if non-linear mode structure modifications are ignored, the model is similar to the HAGIS model [21], at least in the limit when only one perturbation is considered. For a multi-mode system, the relative amplitude change between different modes is ignored so far, however, this is in line with a quasi-linear model where mode saturation amplitude and effective linear growth rates are directly correlated. It should be remarked, that whereas eqn. 1 deals explicitly with fluxes in CoM space, the equation can also be cast as an advection-diffusion equation in the quasi-linear limit [17]. By determining the autocorrelation time τ_{ac} (note that the resonance conditions for all CoM positions and the damping/growth rates for the perturbations are known) the diffusion coefficients can be readily calculated: $D_{P_\phi,P_\phi} = \langle\overline{\frac{dP_\phi}{dt}}\rangle^2 \cdot \tau_{ac}$, and similar for the energy and mixed diffusion tensor elements. As the particle database contains also all mappings from P_ϕ to various orbit averaged radial coordinates (R, pol. flux, tor. flux), the diffusion coefficients can be transformed to m^2/s units.

Implementation

The newly written ATEP code is technically closely interlinked with well-established IMAS (Integrated Modelling and Analysis Suite) framework and its data structures [18]. It profits in design and modularity from the recently established EP-Stability workflow (WF) that is used in this paper to calculate the linear mode spectrum [19]. The interfaces between the different codes employ IMAS data structures, meaning that all operations needed to set up the ingredients for the PSZS evolution equations are in principle replaceable by equivalent codes or models.
Using the linear gyrokinetic mode information (radial structure, frequency, damping/growth rate) as

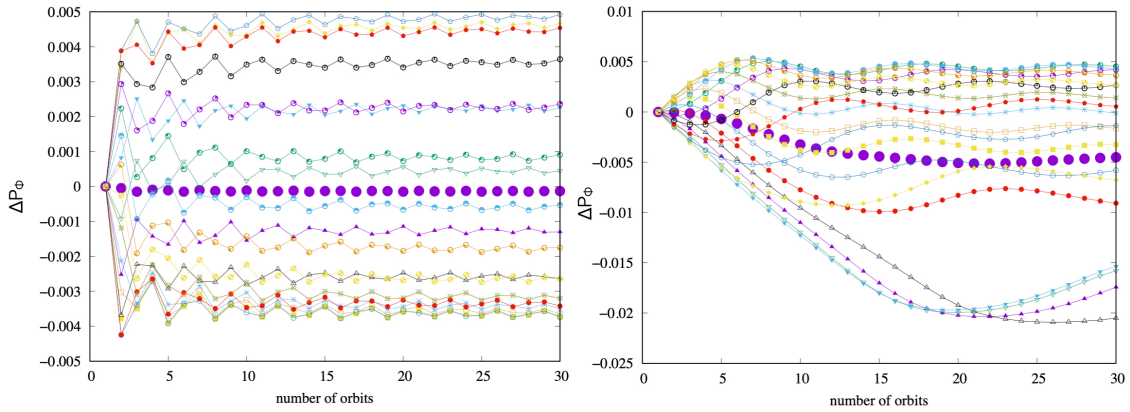

Figure 1: *Ensemble of particles with different toroidal phases (different colors) with respect to an* $n = 13$ *TAE at fixed amplitude (*$\delta B/B = 5 \cdot 10^{-4}$*) representing one point in CoM space: on the left (*$P_\phi = -0.015$*,* $E = 200keV$*,* $\Lambda = 0.0017$*) the passing particles are non-resonant, the average* $\Delta P_\phi = P_{\phi,t} - P_{\phi,start}$ *is vanishing. On the right (*$P_\phi = -0.015$*,* $E = 200keV$*,* $\Lambda = 0.84$*) the barely passing particles are resonant. For not too large perturbations,* ΔP_ϕ *initially grows proportional to the number of transits, at later times the particles have been 'transported' and remain at their final position. For typical parameters* $\delta B/B < 1...5 \cdot 10^{-3}$ *averaging over 5 orbits leads to accurate and reasonably fast results for* $\langle \overline{\Delta P_\phi / dt} \rangle$*. The phase averaged* P_ϕ *is plotted as well (full dots). Note that* P_ϕ *here is normalised to* $Ze\psi$ *with* ψ *the poloidal magnetic flux at the last closed flux surface.*

given by the LIGKA code[20] embedded in the EP-Stability WF, the well-established HAGIS code [21] is employed to calculate the response $\langle \overline{dP_\phi/dt} \rangle$ and $\langle \overline{dE/dt} \rangle$ for a set of pre-selected sample markers for different perturbation amplitudes. First, a set of markers covering the whole CoM space, including co- and counter-passing particles is generated by a code wrapper called 'finder' with a prescribed grid CoM resolution ($128x40x40$ in this paper). The grids are refined close to the trapped passing boundary, and all orbits properties such as topological status, transit time, averaged precession drift and average radial position are determined by following all particles for one orbit in the equilibrium configuration. After that a perturbation (or set of perturbations) is added at a fixed amplitude $\delta B/B$, and the markers are followed for $N = 5 - 10$ orbits (see fig. 1). In addition, each marker in CoM space is replaced by 10-20 identical markers that are started with a different phase in the toroidal angle $2\pi/n_{tor}$, where n_{tor} is the toroidal mode number of the perturbation. For a multi-mode case the lowest toroidal mode number is typically used, or a random phase seed can be chosen. This procedure is a very effective zonal and orbit average procedure, since now $\langle \overline{dP_\phi/dt} \rangle$ for each marker can be recorded, and averaged over N orbit transits (as the individual transit times are known) and all toroidal angles. At the same time also $\langle \overline{dE/dt} \rangle$ is calculated. As expected a linear relation between $\langle \overline{dP_\phi/dt} \rangle$ and $\langle \overline{dE/dt} \rangle$ is found due to the conservation properties of the wave-particle system. This averaging procedure removes the n_{tor}-dependent part of the particle response, as described in the theoretical framework. It should be noted that the dynamics of strongly unstable perturbations with ballistic transport (i.e. particles remain only a fraction of their individual orbits in the perturbations' potential) is not properly captured. However, as we aim to construct a transport model for long time scales, this type of physics is ignored for now. In order to quantify the simplifications related to this procedure, a connection to detailed analyses of transport scaling laws (diffusive/convective) for both Alfvénic gap and energetic particle modes using Lagrangian coherent structures is in progress [22, 23]. The 'finder' tool is also used to calculate orbit-averaged collision coefficients, using the collisional version of the HAGIS code [16, 24].

The calculated transport coefficients can be projected onto the final 3D CoM grid used in the ATEP code (typically 64 to 96 grid points per P_ϕ, E, Λ and mode amplitude, but higher resolutions are possible). A multi-level spline interpolation algorithm [25] is used in order to set up $\mathbf{v}_{P_\phi,E}(\delta B/B)$ from

the somewhat scattered (loss boundaries, refinement at trapped passing boundary) HAGIS data on the regular CoM grid. The results are shown in fig. 2 where co and counter-passing CoM grids have been separated [26], however the trapped grid is kept for both cases in order to ensure smooth splining across topological boundaries. Main and higher-order resonances can be seen, showing the phase-space dependent transport properties of a resonant toroidal Alfvén eigenmode (TAE) perturbation. Obviously, any projection to a lower dimensional transport coefficient would neglect energy and pitch angle dependencies that turn out to be especially important for the calculation of zonal currents.

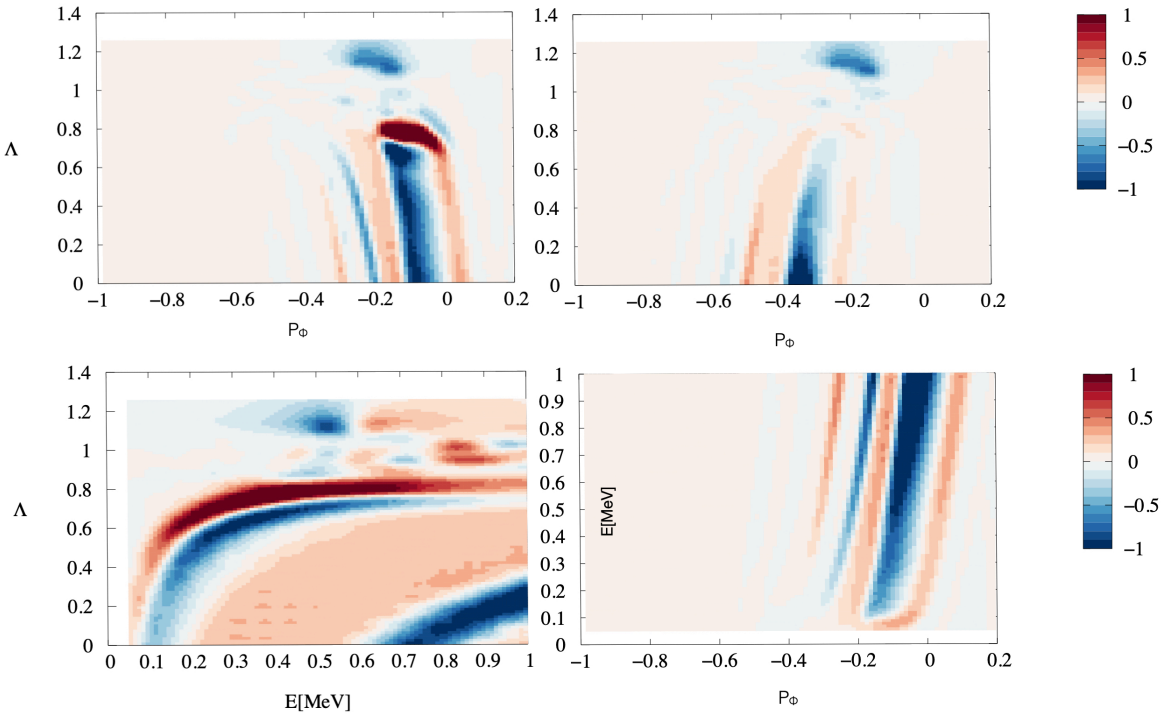

Figure 2: $\langle \overline{dP_\phi/dt} \rangle$ *for a single* $n = 13$ *TAE with* $\delta B/B = 5 \cdot 10^{-6}$ *as a function of the CoM space for different slices: left top: co-passing and trapped particles, right top: counter-passing and trapped particles for* $E = 500keV$*. Bottom left: E-*Λ *plane with* $\Lambda = \mu B_0/E$ *for* $P_\phi = -0.2$*; bottom right:* P_ϕ*-E plane for* $\Lambda = 0.12$ *(deeply passing particles). Blue/red colors refer to outward/inward transport (negative/positive* P_ϕ *direction). Note that* P_ϕ *is normalised to* $Ze\psi$ *with* ψ *the poloidal magnetic flux at the last closed flux surface.*

In this paper we use the METIS generated ITER pre-fusion scenario simulation #100015/1, and a set of TAE modes with toroidal mode numbers $n_{tor} = 13, 14, 15$. For this simulation three different neutral beam generated EP distribution functions (hydrogen) as calculated by the NEMO/SPOT WF [27] are available: one with both beams on-axis, one with both beams off-axis and a mixed on-off-axis case. The NEMO/SPOT results are stored as set of markers in the IDS *distribution*, containing the complete set of spatial and velocity coordinates, together with the canonical CoM coordinates and the marker weights. Clearly, any other code giving the same information can be readily used as input. The marker data is imported into the ATEP code similarly to the $\mathbf{v}_{P_\phi,E}(\delta B/B)$ data. Depending on the marker resolution, binning, smoothing and splining of this original F_{EP} is required. Obviously, there is some arbitrariness in this process. Here, we first bin the markers into the regular CoM grid described above, and then construct a 2D spline in each of the sub-spaces (P_ϕ, E) , (P_ϕ, Λ) and (E, Λ). Individual smoothing can be applied for each of the sub-grids. Then, a 3D spline is constructed and the derivatives with respect to P_ϕ and E are determined. The result can be seen in fig 3.

After these preparation steps eqn. 1 can be evolved in time. Being a 'simple' advection (diffusion) problem, standard methods in the literature can be used. So far we employ an explicit 2nd order Lax-Wendroff-scheme with automatic time step adoption (Courant-limit check) and a Matlab based

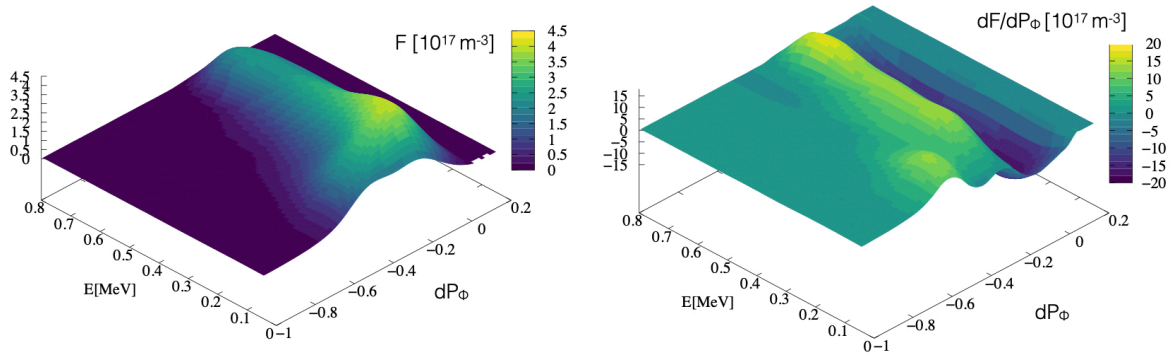

Figure 3: *Distribution function of energetic hydrogen particles,* #100015/1*, in ITER's off-off-axis beam configuration. The original marker data as calculated by the NEMO/SPOT package was binned, smoothed, splined and projected onto the regular CoM grid of the ATEP code (slice with* $\Lambda = 0.5$*)*

implicit Crank–Nicolson solver for testing. A final choice of the solver (including parallelisation and performance optimisation) will be made at a later time.
The preparation of the input for ATEP requires moderate computational effort: depending on the model, the runtime for EP-Stability WF is a couple of seconds to a few minutes [19]. Preparing the orbit- and zonally-averaged data requires typically 15 minutes on 32 cores (ITER SDCC cluster). Although this step is already parallelised it can be further optimised and accelerated in the future. Reading, binning and splining requires about 30 seconds (depending on the CoM grid). Finally, transport steps are quite fast, however the Courant criterion for the explicit solver may require small time steps. The implicit solver [16] resolves this problem, but still needs parallelisation for larger CoM grids. The time-advanced F_{EP} on the CoM grid is remapped into the marker-space via updating the individual weights of markers belonging to a certain CoM position according to the change of phase space density at that position. It becomes obvious, that the markers themselves are not transported, just their weights are evolved according to the PSZS fluxes. Then, standard averages and moments can be taken to determine density, current and pressure in physical units. This information (or the EP diffusion coefficients discussed above) can be passed to a comprehensive transport code. In summary, all ingredients for solving the PSZS transport equation and its interfaces to other transport codes have been established. For details on the collisional part please refer to ref. [16].

First results

As in fig. 2 we use the even $n = 13$ TAE at various fixed amplitudes to evolve the system, i.e. eqn 1. At each time step, the energy of F_{EP} is determined via integrating over CoM space and normalising to the initial energy E_0: $\mathscr{E}(t) = \int dv_{P_\phi,E,\Lambda} E \cdot F_{EP}(t)/E_0$. Density conservation is enforced, as in this case no outflux from the CoM grid is allowed. So far, the term $F_z \frac{\partial}{\partial P_\phi} \langle \overline{\frac{dP_\phi}{dt}} \rangle$ in eqn. 1 is omitted (similar for the E-term), assuming that it is negligible in the kick-model limit. Losses and transport to thermal energies (the energy boundary was set to 50 keV) are ignored so far. As one can see in plot 4, the total energy stored in F_{EP} is decreasing due to the PSZS fluxes. That means that the perturbation is able to extract energy from the gradient of F_{EP}, as it is expected for an unstable TAE. Note, that for perturbations that are not consistently chosen as unstable eigenmodes of the system, the total energy can also increase, meaning that the perturbations increase $\mathscr{E}(t)$. In this example $\mathscr{E}(t)$ decreases linearly in the first phase, its linear 'damping' rate being proportional to the applied $\delta B/B$. Plotting the same data $1 - \mathscr{E}(t)$ on a $\log t$ scale shows how the same amount of energy is extracted on very different time scales for different $\delta B/B$. As the perturbation amplitude is held fixed, at some point the free energy is exhausted, and the total energy reaches a minium. As $\delta B/B_0$ remains fixed in the kick model limit and damping is ignored, the phase space density is further 'advected'. This requires energy, and thus the

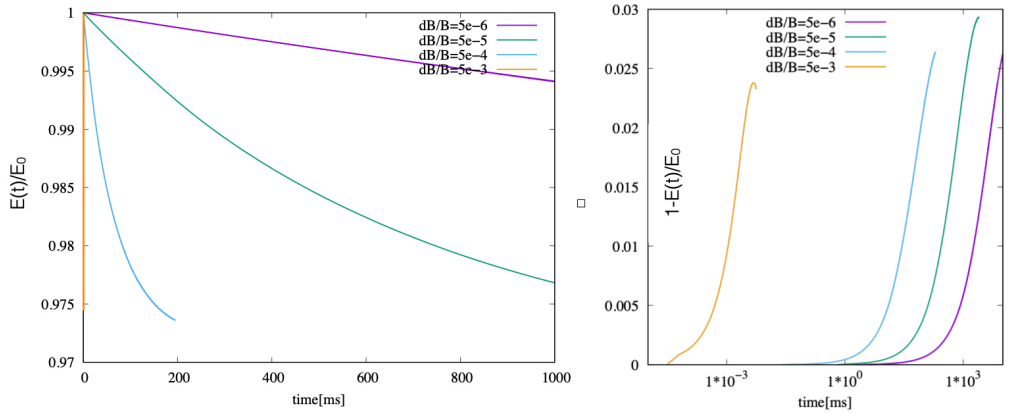

Figure 4: *Linear (left) and logarithmic (right) time evolution of the normalised total energy* $\int dv_{P_\phi,E,\Lambda} E \cdot F_{EP}(t)/E_0$ *using the kick model limit for* #100015/1*, in ITER's off-off-axis beam configuration for a fixed TAE with different amplitudes.*

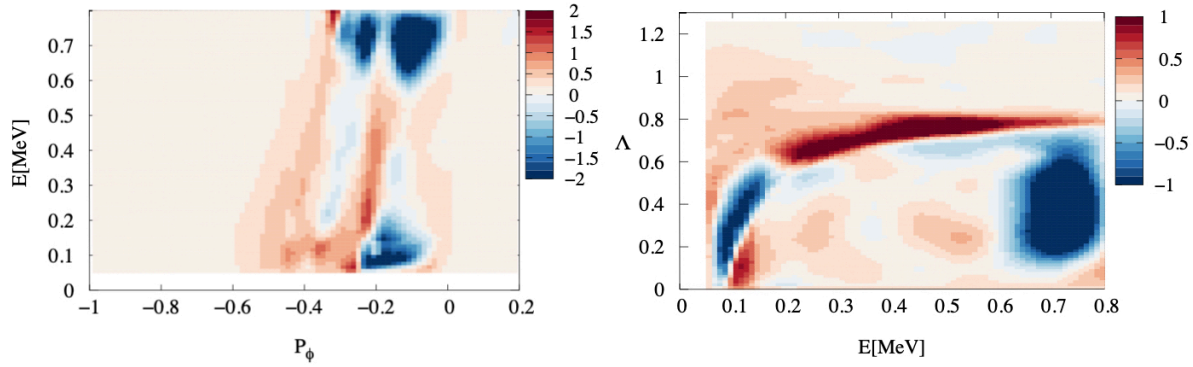

Figure 5: *Left: the PSZS state* $\delta F_{EP} = F_{EP}(t = 700ms) - F_{EP}(t = 0)[10^{16} m^{-3}]$ *for* #100015/1 *(off-off-axis beam configuration) in the kick model limit with* $\delta B(t)/B) = 10^{-5}$ *in* (P_ϕ, E) *plane, integrated over* Λ *; right:* $\delta F_{EP}[10^{16} m^{-3}]$ *in* (E, Λ) *plane integrated over* P_ϕ*. Here,* F_{EP} *as shown in fig. 3 was used.*

total energy starts to increase again. Including sources and collisions [16] balancing the EP transport will lead to consistent saturation levels. We can use the minimum in $\mathscr{E}(t)$ to define a maximally relaxed state. In fig. 5 such a relaxed zonal state $\delta F_{EP} = F_{EP}(t) - F_{EP}(t = 0)[10^{16} m^{-3}]$ is plotted in two different projections. One can see that - as expected - the transport is mainly radially outwards (negative P_ϕ being outwards). Also, high-energy phase space density is reduced and lower-energy regions more strongly populated. This illustrates how different CoM regions of the beam F_{EP} drive and damp the perturbation, i.e. how EP energy is channeled on average via Landau damping to low-energy regions (α-channeling [28]). Projecting F_{EP} from the CoM grid back to real space and taking moments allows us to determine the zonal density and the zonal current that represent the radial transport of EP density and current, as plotted in fig. 6. One can see how F_{EP} is relaxed, i.e. the gradients flattened and EP density and current are transported radially outwards, as theoretically expected. Clearly, this information can be used to construct a new non-linear equilibrium, and by using a sensible iteration scheme, the ATEP code can be cast into to a reduced EP transport model. As described above, this model can be improved by evolving the wave energy consistently with the change of $\mathscr{E}(t)$. To this end, a set of $\mathbf{v}_{P_\phi,E}(\delta B/B)$ for $\delta B/B) = [10^{-6}, 10^{-5}, 10^{-4}, 10^{-3}]$ is prepared as described above. A 4D spline (3 CoM coordinates and $\delta B/B$) is constructed. Whereas the amplitude dependence is simple for a single mode (essentially the orbit width of the EPs determine the volume of CoM space that is affected by the spatially fixed perturbation), resonance overlap criteria for multi-mode cases can be accurately taken into account by this procedure (details not shown here). Using the fact that the wave

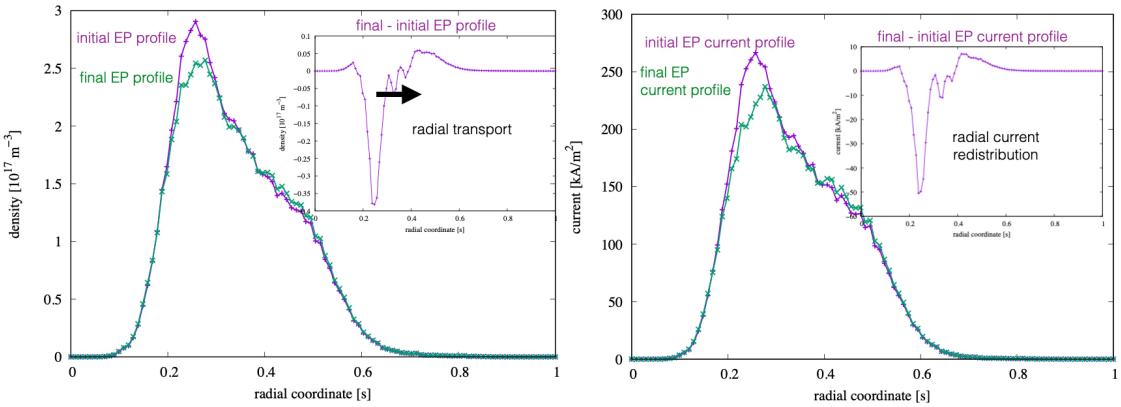

Figure 6: *Left: Radial projection (ρ_{tor}) of the distribution function of energetic hydrogen particles, #100015/1, in ITER's off-off-axis beam configuration, initial (as given by NEMO/SPOT) and final state after evolving the PSZS transport equation for 700ms (1000 time steps) in the kick model limit with $\delta B(t)/B) = 10^{-5}$; right: the initial and final EP-current for the same case. The inlets in both plots show the difference of the final and the initial state.*

energy is $\sim (\delta B/B)^2$, one can map the change of $\mathscr{E}$ for a small initial perturbation to $(\delta B(t)/B)^2$, leading to a stronger initial growth of the perturbation until a saturated $\delta B_{max}/B$ is reached (see fig. 7). Since no damping is included so far, the mode decays only very slowly due to the growing imbalance of beam damping and drive. Including realistic background damping rates will allow us to reach reasonable saturation amplitudes, in line with the nonlinear wave-particle interaction model implemented in HAGIS.

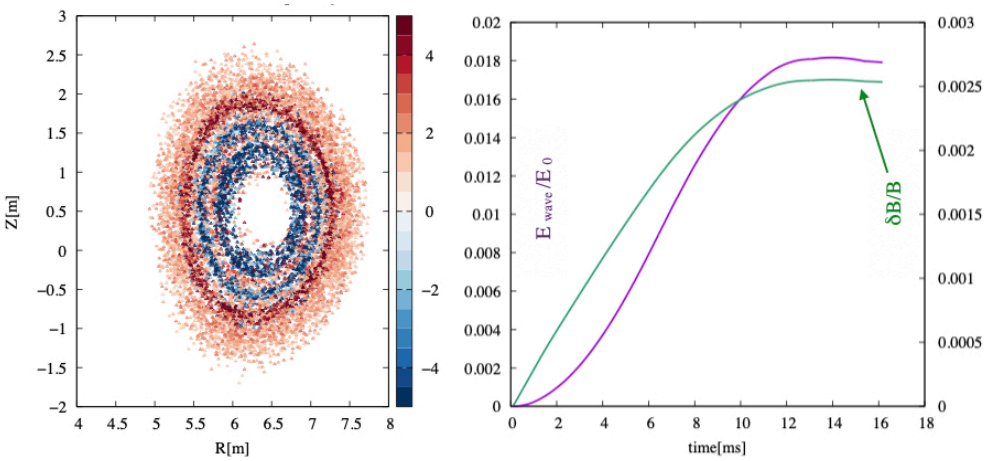

Figure 7: *Left: For the same case as shown in fig. 5: mapping back the PSZS to marker space shows that the transport equation indeed introduces a zonal density perturbation to F_{EP}, here represented as the change of marker weights [%] (color bar). For this plot only the most resonant particles with $E > 500keV$ and $\Lambda < 0.3$ were chosen. Right: the normalised wave energy $E_{wave}(t)/E_0$ and $\delta B(t)/B$ are allowed to evolve dynamically according to the energy balance eqn. 2. After an initial growth phase, saturation and a starting decay is observed.*

Conclusions and outlook

After these first encouraging results, a thorough validation effort will be carried out, profiting from ongoing work within the Eurofusion Enabling Research Project 'ATEP'. To that end comparisons with other reduced models will be carried out, e.g. with an ongoing extension of the DAEPS code

[29, 30, 9] that uses explicit analytical expressions for calculating the phase space fluxes. Also a 1d reduced model based on the beam-plasma bump-on-tail paradigm that is designed to go beyond the quasi-linear approximation and thus forecast possible EP transport transitions such as avalanching[22] will be used to determine the limits of the ATEP model. As mentioned above, its formulation allows one to carry out detailed analysis of transport scaling laws (diffusive/non-diffusive) using Lagrangian coherent structures (LCS) [22, 23]. Further verification and validation is being carried out using comprehensive numerical codes in the appropriate limits (HYMAGYC, (X)HMGC, STRUPHY, ORB5, HAGIS/LIGKA; for a recent benchmark of these codes refer to ref. [4, 31]). To that end, the implementation of PSZS diagnostics in the various codes [32, 33] provides a natural connection point for detailed comparisons. In addition, the Hamiltionian mapping method, as pioneered within the HMGC code, gives further valuable insight into trapping/detrapping processes in single and multi mode systems [32, 34] building on the same LCS methods developed for the 1d beam-plasma model. A new hybrid MHD-kinetic model (STRUPHY) has been developed and implemented [35] as part of the ATEP project. It follows a stringent mathematical formulation using the exterior calculus framework leading to improved non-linear stability behaviour as needed for transport time scale simulations. After validation the ATEP model will be extended to include non-linear interactions via direct and in-direct (i.e. mediated by ZS) coupling mechanisms as described in refs. [7, 8, 9, 10]. Several time-dependent scenarios from present-day and future experiments (particularly AUG, JT-60SA, TCV, DTT, JET, ITER) have been already collected and ported into IMAS for validation and uncertainty quantification. Motivated by the particular needs of the ATEP project for validation cases, dedicated experiments at AUG have been designed and carried out. Building on previously developed scenarios that maximise the ratio of EP vs. background pressure [36], strongly EP-driven mode activity and EP transport in plasmas with different isotope mixes have been observed and are presently analysed.

Acknowledgements. - This work has been carried out within the framework of the EUROfusion Consortium, funded by the European Union via the Euratom Research and Training Programme (Grant Agreement No. 101052200-EUROfusion), within the framework of the Enabling research project 'ATEP'. The views and opinions expressed herein do not necessarily reflect those of the European Commission. ITER is the Nuclear Facility INB no. 174. The views and opinions expressed herein do not necessarily reflect those of the ITER Organisation.

References

[1] A. Mishchenko et al, Proc. 29th IAEA FEC, London UK (2023)
[2] T. Hayward-Schneider et al, Proc. 29th IAEA FEC, London UK (2023)
[3] A. Biancalani et al, Proc. 29th IAEA FEC, London UK (2023)
[4] G. Vlad et al, Proc. 29th IAEA FEC, London UK (2023)
[5] Z. Lin et al, Proc. 29th IAEA FEC, London UK (2023)
[6] A. di Siena et al, PRL **125** (2020)
[7] F. Zonca et al, New Journal of Physics **17** 013052 (2015)
[8] M V Falessi et al, Phys. Plasmas **26** 022305 (2019)
[9] M V Falessi et al, Proc. 29th IAEA FEC, London UK (2023)
[10] M V Falessi et al, NJP submitted https://arxiv.org/abs/2306.08642 (2023)
[11] R.E. Waltz and E.M. Bass, NF **54** 104006 (2014)
[12] M. Podesta et al et al, PPCF **56** 055003 (2014)
[13] N. Gorelenkov et al, NF **58** 082016 (2018)
[14] A. Zocco et al, JPP **89** 905890307 (2023)
[15] A. Kaufman, Phys. Fluids **15** 1063 (1972)
[16] G Meng et al, Proc. 29th IAEA FEC, London UK (2023)
[17] L. Chen et al, JGR **104** 2421 PoP (1991)
[18] F. Imbeaux et al, NF **55** 123006 (2015)
[19] V.-A. Popa et al, NF accepted (2023)
[20] Ph. Lauber et al, J. Comp. Phys., **226/1** (2007)
[21] S.D. Pinches, Comp. Phys. Comm., **111** (1998)
[22] N. Carlevaro et al, Proc. 48th EPS Conference on Plasma Physics, (2022)
[23] A. V. Milovanov et al, Phys. Rev. E **103** 052218 (2021)
[24] A. Bergmann et al **8** 5192 PoP (2001)
[25] S. Lee et al, IEEE Transactions on Visualization and Computer Graphics, **3** (1997)
[26] A. Bierwage et al, CPC **275** 108305 (2022)
[27] M. Schneider et al, NF **61** 126058 (2021)
[28] N. Fisch et al **69** 612 PRL (1992)
[29] Y. Li et al, PoP **27** 062505, (2020).
[30] Y. Li et al, submitted (2023)
[31] G. Vlad et al, Nucl. Fusion **61** 116026 (2021); Proc. 29th IAEA FEC, London UK (2023)
[32] S. Briguglio et al, PoP **21** 112301 (2014)
[33] A. Bottino et al, J. Phys.: Conf. Ser. **2397** 012019 (2022)
[34] X. Wang et al, PoP. **29** 032512 (2022)
[35] F. Holderied et al, JCP **433** 110143 (2021); **464** 111329 (2022)
[36] Ph. Lauber et al, Proc. 27th IAEA FEC (2018)